LCLS-II BUNCH COMPRESSOR STUDY: 5-BEND CHICANE*

D.Z. Khan[#], T.O. Raubenheimer, SLAC, Menlo Park, CA 94025, USA

Abstract

In this paper, we present a potential design for a bunch compressor consisting of 5 bend magnets which is designed to compensate the transverse emittance growth due to Coherent Synchrotron Radiation (CSR). A specific implementation for the second bunch compressor in the LCLS-II is considered. The design has been optimized using the particle tracking code, ELEGANT [1]. Comparisons of the 5-bend chicane's performance with that of a symmetric 4-bend chicane are shown for various compression ratios and bunch charges. Additionally, a one-dimensional, longitudinal CSR model for the 5-bend design is developed and its accuracy compared against ELEGANT simulations.

INTRODUCTION

The Linac Coherent Light Source (LCLS) at SLAC has shown tremendous success in its scientific capabilities in the biological, chemical, atomic and material sciences [2, 3, 4]. To build upon the success of the LCLS, a myriad of upgrades will be made to push the limits of current x-ray free-electron laser (X-FEL) design and technology to meet the ever growing demands of the scientific community. LCLS-II is an upgrade of the LCLS based on a 4 GeV superconducting RF linac [5]. Among the many upgrades being researched, one of particular interest is the bunch compression system.

Compression of electron beams is important in FELs to minimize the gain length [6]. A successful compression system is one that compresses the bunch longitudinally while preserving the beam's transverse emittance. The currently planned compression system of LCLS-II, and many current X-FEL facilities such as FLASH (DESY) [7] and SACLA (RIKEN) [8], uses a sequence of magnetic chicanes to compress the bunch length by orders of magnitude [5]. LCLS-II's two-stage compression (Fig. 1) is simple and effective but poses problems towards the end of its compression cycle via CSR's dilution of horizontal emittance.
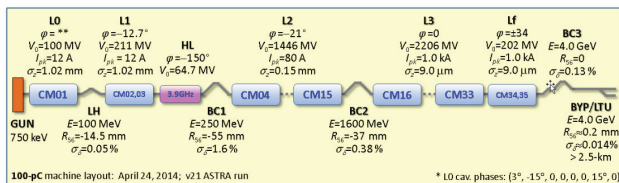
Figure 1: A diagram of the LCLS-II beamline with relevant component details. LCLS-II plans to utilize a two-stage magnetic chicane compression system; BC1 and BC2. The topic of this paper focuses on the self-radiative effects of the electron beam experienced in BC2.

On the curved sections of an FEL beamline the electron beam can interact with itself. The synchrotron radiation from the electrons in the tail of the bunch can interact with the electrons in the head under the right conditions. The phenomenon becomes highly disruptive when the phase difference between the radiating electrons is small i.e. when the bunch length becomes comparable to the radiation wavelength. Under this regime, the synchrotron radiation becomes coherent and its power scales as N^2, where N is the electron population of the bunch. In the coherent regime, the radiation causes a strong non-linear longitudinal energy chirp. This chirp can be estimated using a simple 1-D model [9]:

$$\frac{dE}{ds}(z) = \int_{-\infty}^{z} \frac{d\lambda(z')}{dz'}\left(\frac{1}{(z-z')^{\frac{1}{3}}}\right)dz' \qquad (1)$$

$$\sigma_{RMS-\delta} = 0.22\frac{r_e N L_B}{\gamma \rho^{2/3}\sigma_z^{4/3}} \propto [L_B^{\frac{1}{3}}][\theta^{\frac{2}{3}}][\sigma_z^{-\frac{4}{3}}] \qquad (2)$$

where z is the longitudinal position along the bunch, λ is the normalized electron distribution, L_B is the magnet length, ρ is the bending radius and σ_z is the RMS bunch length. Equations 1 and 2 are derived from a 1-D model of the steady-state CSR wakefield. The CSR effect can create a number of unwanted effects on the electron beam [10, 11]. In this paper, we concern ourselves namely on CSR's influence on the bend plane's projected emittance growth.

Novel techniques have been developed to mitigate and nullify the CSR effect. Adjusting the linac optics to provide a $-I_{2x2}$ transfer matrix between two sequential bends (such as in doglegs) has shown to provide excellent cancellation of CSR induced emittance growth [12]. A main assumption of this method is that the bunch length of the beam is constant between successive bends and therefore, the CSR RMS energy spread can be assumed to be identical at each location. The matter becomes highly complicated when the bunch length between the two successive bends is evolving, such as that of the bunch compressor. For an evolving bunch length, studies have shown that a minimization of the $\mathcal{H}$-function in CSR significant bends results in significant reduction of emittance growth [13]. Compressor designs based on matched chicanes or large period wigglers can also reduce the emittance growth [14, 15]. Utilizing asymmetry in a chicane design (allocating more R_{56} in the first half of a, for example, 4-bend chicane) has shown success in partial nullification of emittance dilution when compared to the standard symmetric designs [16, 17]. Additionally, it has been shown that, in multi-stage compression systems, allocating more R_{56} to the initial bunch compressors, while maintaining final compression, dampens the CSR effect in the final compressor where CSR is most detrimental [13]. Though the techniques cited

demonstrate effective reduction of the CSR induced emittance dilution, they tend to require many additional magnetic elements that can lead to further degradation of the longitudinal phase space and fall short of complete nullification.

LCLS-II CURRENT BUNCH COMPRESSOR

The currently planned compression scheme of LCLS-II consists of a two-stage magnetic chicane system. Each compressor is comprised of the standard 4-bend chicane (Fig. 2). We focus our attention on the second bunch compressor (BC2) where the CSR is most influential. Pertinent details of the BC2 are included in table 1.
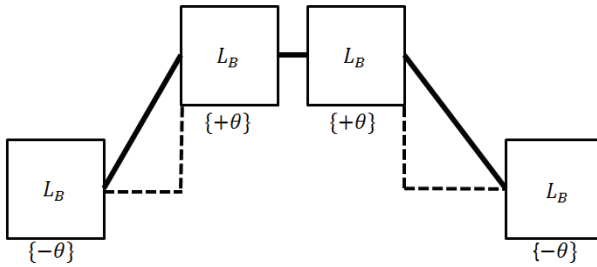
Figure 2: A cartoon of the 4-bend chicane being used for BC1 and BC2 at LCLS and currently planned for LCLS-II.

Table 1: Various Design Parameters of BC2 in LCLS-II

Parameter	Symbol	BC2	Unit
Electron Energy	E_0	1.6	GeV
Momentum Compaction	$|R_{56}|$	59.9	mm
Chicane Total Length	L_T	23.0	m
Bend Angle Per Dipole	$|\theta|$	0.05	Rad
Eff. Length Of Each Bend	L_B	0.54	m
Dispersion At Center	$|\eta_x|$	562	mm

To gain greater insight on the CSR mechanism of BC2 we used ELEGANT to generate phase space plots of the longitudinal momentum change along the bunch as it evolves through BC2. From Figure 3, we see the CSR

wakefield begins to become significant in the third bend and fourth bends.

For a simplistic understanding of the emittance growth, we employ a linear kick model for the CSR [12]. The linear kick model provides a useful approximation of the CSR's effect on the bend plane emittance in terms of first-order energy kicks (Eq. 2) to the beam's centroid at each dipole's center. With the energy kicks, one can calculate the associated spatial (Δx) and angular ($\Delta x'$) kicks at the ith dipole given the local dispersion and dispersion's slope:

$$\Delta x_i = \eta_i \delta_P = \int R_{16i}(s)\, \delta_i ds \qquad (3)$$
$$\Delta x'_i = \eta'_i \delta_P = \int R_{26i}(s)\, \delta_i ds \qquad (4)$$

For coherent processes, the spatial and angular kicks can be summed linearly at each bend location and the final projected emittance is described by [18]:

$$\epsilon^2 = \epsilon_0^2 +$$
$$\epsilon_0 \sqrt{\beta (\sum \Delta x'_i)^2 + 2\alpha \sum \Delta x_i \sum \Delta x'_i + \gamma (\sum \Delta x_i)^2} \qquad (5)$$

Applying the linear kick model to the 4-bend chicane of BC2 allows us to see the limitations of the compressor and investigate a new compressor set up in regards to full emittance growth cancellation. Naturally, from equation 5, we see that a route to emittance growth cancellation is to have the kick sums cancel. With equations 3 and 4, we can develop a relation for the sum of spatial and angular kicks in the final two bends of BC2 where CSR is significant:

$$\sum \Delta x = \theta_B (L_B + L_D) \delta_{P3} \qquad (6)$$
$$\sum \Delta x' = \theta_B (\delta_{P3} + \delta_{P4}) \qquad (7)$$

where θ_B, L_B, L_D, δ_{P3}, and δ_{P4} is the bend angle, bend length, drift length between the 3rd and 4th bend, and the CSR RMS spread in bend 3rd and 4th bend, respectively. From equations 6 and 7, we see that the kick sums mathematically cannot cancel for the 3rd and 4th bends; they can only be minimized. Though, with the design constraints of maintaining R_{56} and having no residual dispersion at the exit of the 4th bend (achromatic condition), we begin to realize the limitations of the CSR emittance growth cancellation of the 4-bend chicane.
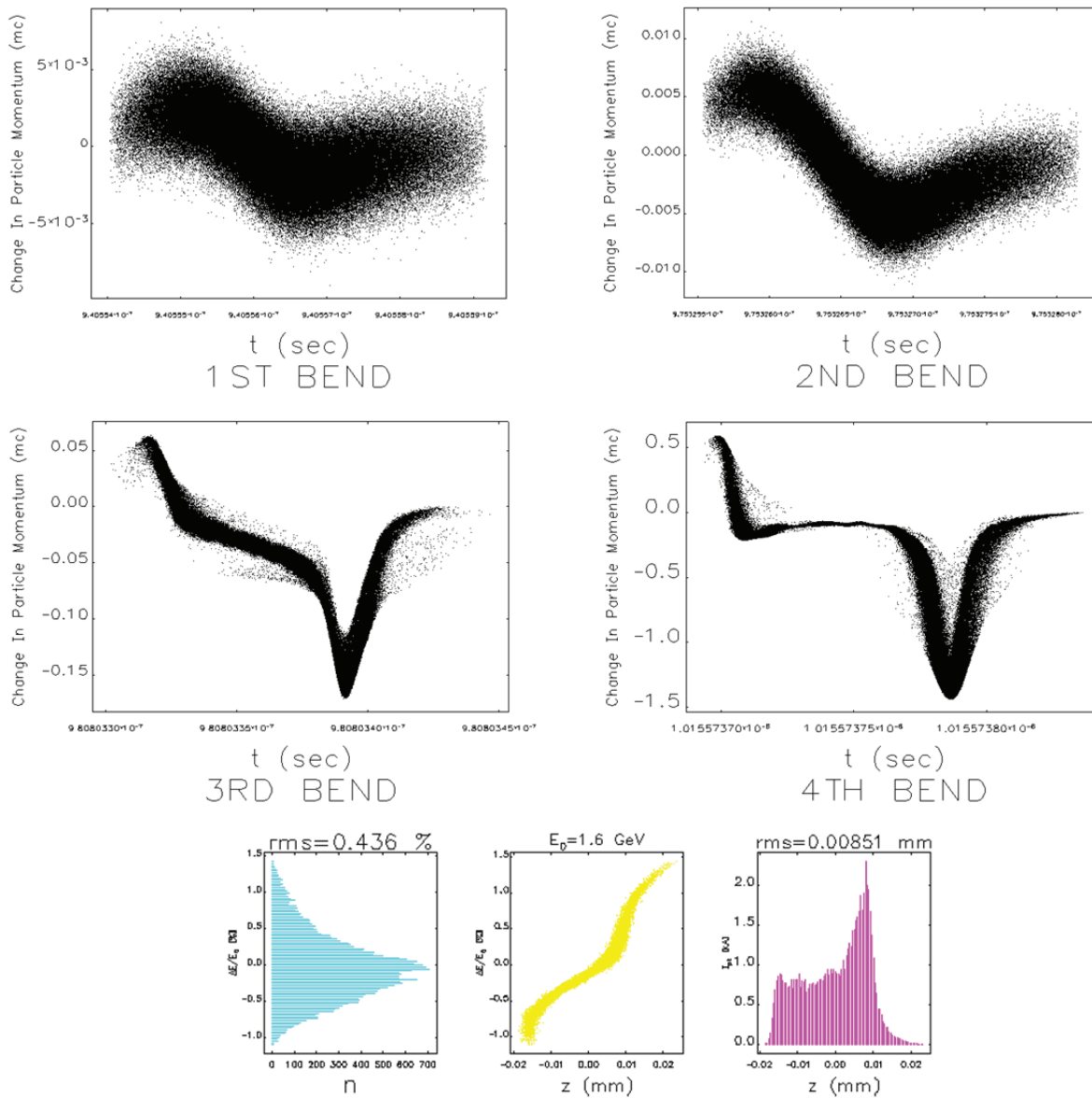
Figure 3: Top/Middle: The momentum difference for each particle in each bend in the planned LCLS-II BC2 4-bend chicane generated with ELEGANT. The CSR wake begins to take form in the third bend where the bunch is compressed to 7 microns. Bottom: (From left to right) The normalized energy spread, longitudinal energy phase space, and the current profile of the beam at the exit of BC2.

LCLS-II PROSPECTIVE BUNCH COMPRESSOR

The prospective chicane design (Fig. 4) is based on the aforementioned studies in this paper. If we are to design a compressor that has transverse spatial and angular kicks cancel, we consider the following:

1. The CSR energy kick is heavily weighted by the bunch length. As the bunch length decreases, the CSR energy kick increases to the inverse 4/3 power (Eq. 2).

2. The bend length and angle play a secondary role in the CSR energy kick. Decreasing either parameter will decrease the CSR energy kick to the 1/3 and 2/3 power, respectively (Eq. 2).

3. The spatial and angular kick directions are entirely dependent on the local dispersion. The 4-bend chicane creates a solely polarized dispersive region which limits the cancellation potential of the kicks. An extra, oppositely directed dispersive region should be added to the chicane to allow the kicks to cancel.

4. The large bunch length makes the CSR nearly negligible in the first two bends in comparison to the last two. The angles of the first two

bends can be increased, while maintaining R_{56}, without much CSR induced consequences.

With these tenants in mind, we implement changes to the 4-bend chicane with the goal of completely cancelling the CSR induced emittance dilution.
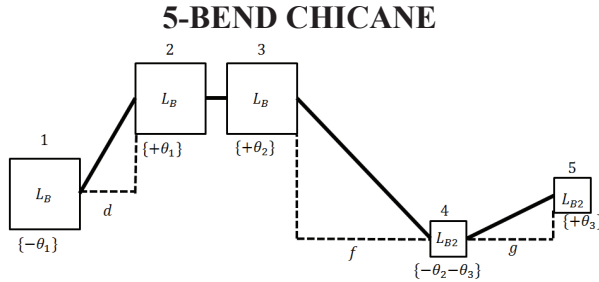
5-BEND CHICANE

Figure 4: The 5-Bend Chicane. A second stage bunch compressor exhibiting full CSR induced emittance growth cancellation.

Table 2: The Various Characteristic Parameters of the 5-Bend Chicane Compared with the 4-Bend Chicane for BC2

Parameter	Symbol	5-Bend Chicane	4-Bend Chicane	Unit
Electron Energy	E_0	1.6	1.6	GeV
Momentum Compaction	$|R_{56}|$	59.9	59.9	mm
Chicane Total Length	L_T	17.0	23.0	m
First Chicane Drift Length	L_D	3.3	9.8	m
Second Chicane Drift Length	L_F	8.7	N/A	m
Third Chicane Drift Length	L_G	1.7	N/A	m
Magnet 1 Angle	$|\theta_1|$	0.103	0.05	Rad
Magnet 2 Angle	$|\theta_1|$	0.103	0.05	Rad
Magnet 3 Angle	$|\theta_2|$	0.046	0.05	Rad
Magnet 4 Angle	$|\theta_2| + |\theta_3|$	0.060	0.05	Rad
Magnet 5 Angle	$|\theta_3|$	0.014	N/A	Rad
Eff. Length Of Magnet 1, 2, 3	L_B	0.54	0.54	m
Eff. Length Of Magnet 4 & 5	L_{B2}	0.25	0.54	m
Dispersion After Magnet 2	$|\eta_x|$	401	562	mm
Dispersion After Magnet 4	$|\eta_x|$	25	N/A	mm

We decreased the last two bend lengths and angles to account for the decreasing bunch length and to decrease the CSR effect (Table 2). Consequently, we increased the first bend angles to preserve the original compression and R_{56}. An extra bend is added in between the 4-bend's third

and fourth bend to create an extra oppositely directed dispersive region that improves the potential for kick cancellation (Fig. 5b).
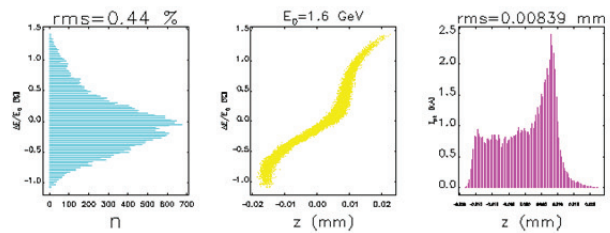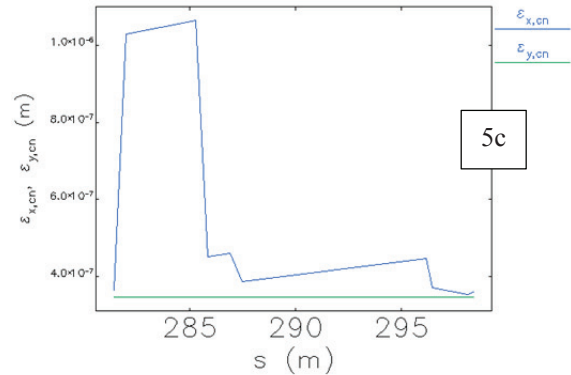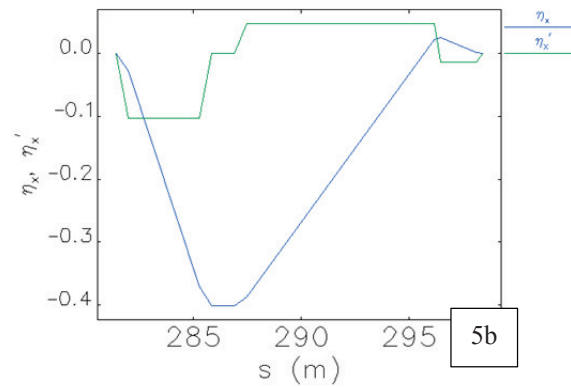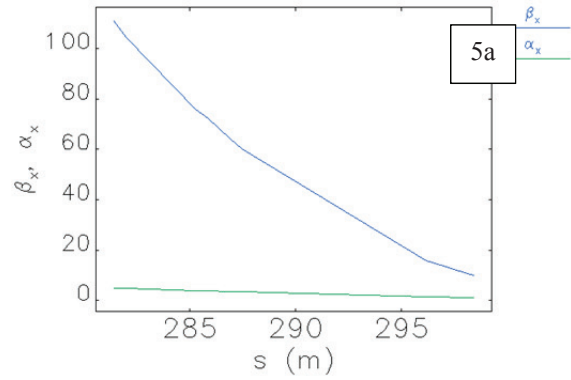
Figure 5 (Top to bottom): 5-bend chicane's: (a) The transverse x-plane β and α functions; (b) The dispersion and slope of dispersion function; (c) The dispersive corrected normalized transverse emittances (ecnx, ecny); (d) The normalized energy spread, longitudinal energy phase space, and the current profile.

A first order approximation of the spatial and angular kicks, such as one previously performed for the 4-bend chicane (Eq. 3 and 4), provides us with the mathematical insight of the 5-bend chicane's emittance dilution suppression:

$$\sum Kicks' = \theta_1(L_B + d)(\delta_{P3} + \delta_{P4}) - \frac{1}{2}\theta_2\left(2f + L_B + \left\{\frac{\theta_2}{\theta_2+\theta_3}\right\}L_{B2}\right)\delta_{P4} \qquad (8)$$

$$\sum Kicks' = \theta_2(\delta_{P3} + \delta_{P4}) - \theta_3(\delta_{P4} + \delta_{P5}) \qquad (9)$$

where, respectively, θ_1, θ_2 and θ_3 are the 1st, 2nd and 3rd bend angles. L_B, L_{B2}, d, and f are the large and small magnet lengths and the 1st and 2nd drift spaces. And, δ_{P3}, δ_{P4} and δ_{P5} are the CSR RMS energy spread for the 3rd, 4th and 5th bending magnets. As with the 4-bend chicane case, the CSR wakefield begins to become significant in the 3rd magnet, so the kicks from the 3rd magnet and onward have been included in the linear kick model calculation. The form of equations 8 and 9, although more complicated than the 4-bend chicane, show more potential in having the kicks cancel.

Simulations performed in ELEGANT, with CSR turned on in the magnets and drifts, show that the 5-bend chicane provides excellent transverse emittance preservation (Fig. 5c). In fact, it has remarkably cancelled all transverse emittance growth due to CSR in the bunch compressor.

DESIGN IMPLEMENTATION & ENGINEERING CONSIDERATION

Although the benefits of the 5-bend chicane is clearly evident, its complexity does provide some difficulties in actually engineering the design [19, 20]:

1. The small magnets in the 4th and 5th bends require large field strengths to achieve their desired bend angle. The 4th bend, in particular, is highly problematic. With a 0.25 m magnet length and 0.060 rad bending angle, it would require a 13 kG field strength.
2. The three unique bending angles of the 5-bend chicane require a complicated powering scheme. A benefit afforded by the 4-bend chicane's simple design is it requires only a single power supply to power all four magnets amounting to a small $\frac{\Delta\theta}{\theta_B}$ deviation error throughout the system. Such is not the case for the 5-bend chicane. The first two magnets can be powered in series, while the three subsequent magnets would require their own power source, greatly increasing the $\frac{\Delta\theta}{\theta_B}$ of the system.

To ease the design and engineering efforts of the 5-bend chicane, we applied the following modifications [19, 20]:

1. Decrease the magnet strengths to provide a 50% overhead on the field requirements (Table 3):

Table 3: Revised Field Strength for each Magnet of the 5-Bend Chicane

Parameter	Symbol	5-Bend Chicane	Unit
Magnet 1	B_1	8.5	kG
Magnet 2	B_2	8.5	kG
Magnet 3	B_3	4.0	kG
Magnet 4	B_4	5.1	kG
Magnet 5	B_5	1.1	kG

2. Use identical magnets for each bend to allow the system to be powered in series just as in the 4-bend case.
3. Alter the coil number and gap size of each magnet to achieve the desired field strength; trim coils can further provide fine tuning.

Implementing these design revisions into the 5-bend design (Table 4) we then have:
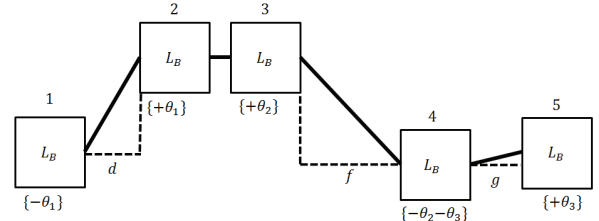
Figure 6: The revised 5-bend chicane with identical magnet lengths and overall decreased bend angles.

Table 4: The Various Characteristic Parameters of the Revised 5-Bend Chicane Compared with the 4-Bend Chicane for BC2

Parameter	Symbol	5-Bend Chicane	4-Bend Chicane	Unit
Electron Energy	E_0	1.6	1.6	GeV
Momentum Compaction	$|R_{56}|$	59.9	59.9	mm
Chicane Total Length	L_T	17.8	23.0	m
First Chicane Drift Length	L_D	4.4	9.8	m
Second Chicane Drift Length	L_F	9.4	N/A	m
Third Chicane Drift Length	L_G	1.3	N/A	m
Magnet 1 Angle	$|\theta_1|$	0.087	0.05	Rad
Magnet 2 Angle	$|\theta_1|$	0.087	0.05	Rad
Magnet 3 Angle	$|\theta_2|$	0.046	0.05	Rad
Magnet 4 Angle	$|\theta_2| + |\theta_3|$	0.060	0.05	Rad
Magnet 5 Angle	$|\theta_3|$	0.014	N/A	Rad
Eff. Length Of Each Bend	L_B	0.54	0.54	m
Dispersion After Magnet 2	$|\eta_x|$	445	562	mm
Dispersion After Magnet 4	$|\eta_x|$	22	N/A	mm

The performance of this revised 5-bend chicane (Fig. 6) is successful in greatly reducing the transverse emittance growth, but not in complete cancellation like before (results in 2.9% increase). Below, in Figure 7, are the relevant emittance and phase space plots of the revised 5-bend chicane from ELEGANT simulations. Comparing the phase space plots to that of the emittance dilution cancelling 5-bend (Fig. 5d) and 4-bend (Fig. 3) chicane, we see that the revised 5-bend chicane preserves the beam phase space extremely well.
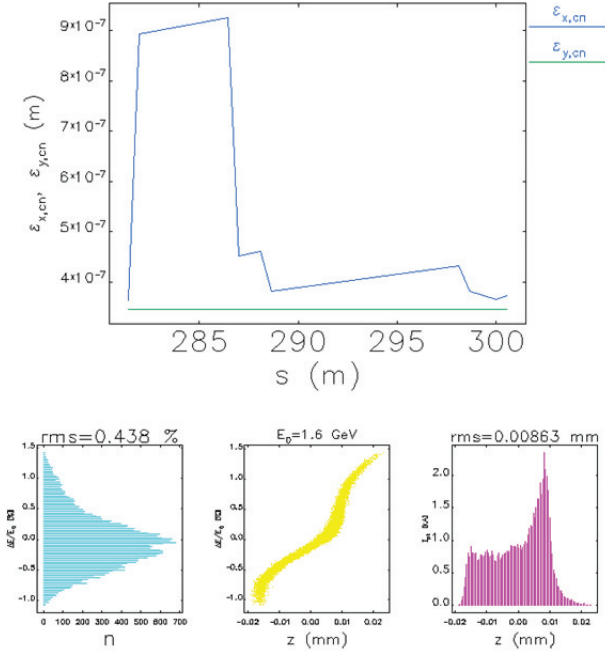
Figure 7: Top: The projected normalized corrected transverse emittance throughout the revised 5-bend chicane. Bottom (From left to right): The normalized energy spread, longitudinal energy phase space, and the current profile.

All discussions leading up this point has been in regards to nominal operations; 100pC bunch compressed to approximately 8.5 microns at the exit of BC2. For a comprehensive performance evaluation of the revised 5-bend chicane we compared its performance with that of the currently planned 4-bend chicane for two common bunch distributions and various compression ratios [21]. The results are displayed in table 5(a, b). The revised 5-bend chicane clearly outperforms the 4-bend chicane in emittance preservation for all cases.

Table 5a: "1.5kA" Chicane Test of BC2 in LCLS-II

Momentum Compaction $|R_{56}|$ (mm)	Final Bunch Length (μm)	4-Bend ϵ_xGrowth (%)	5-Bend ϵ_xGrowth (%)
45.3	5.5	239	8
45.1	6.5	171	5
44.9	7.5	113	3
44.7	8.5	71	3
44.5	9.5	45	2

Table 5b: "1.0kA" Chicane Test of BC2 in LCLS-II

Momentum Compaction $|R_{56}|$ (mm)	Final Bunch Length (μm)	4-Bend ϵ_xGrowth (%)	5-Bend ϵ_xGrowth (%)
36.6	5.5	178	23
36.3	6.5	135	13
36.0	7.5	91	8
35.7	8.5	59	5
35.4	9.5	37	4

LINEAR CSR MODEL

In this section, we develop a numerical treatment of the linear kick model for the emittance dilution cancelling 5-bend chicane, and test its results with that of ELEGANT. We have included the effects of bunch compression by approximating the bunch length as a linear function of angle traversed through the bending magnets [19]:

$$\sigma_z(\theta) \to \frac{\sigma_{zbeg} - \sigma_{zend}}{\theta_B}\theta + \sigma_{zbeg} \qquad (10)$$

where σ_{zbeg}, σ_{zend}, θ_B and θ is the bunch length at the entrance of the magnet, the bunch length at the exit of the magnet, the total bend angle of the magnet and the angle traversed by the bunch into the magnet, respectively. On the treatment of the CSR self-interaction in the system we employ two methods.

Steady State Regime

The CSR self-interaction is considered to be constant throughout the bunch's trajectory in the magnet (the slippage length approaches infinity) and follows the form of equation 1 and its RMS Energy change following equation 2. We can calculate the RMS spatial and angular kicks by integrating the CSR RMS energy change with the dispersion function through the bending magnet as so [18]:

$$< \Delta x_i > = \int R_{16i}(s)\, \delta_{RMS-i}\, ds \qquad (11.a)$$
$$< \Delta x_i^2 > = (\int R_{16i}(s)\, \delta_{RMS-i}\, ds)^2 \qquad (11.b)$$

$$< \Delta x'_i > = \int R_{26i}(s)\, \delta_{RMS-i}\, ds \qquad (12.a)$$
$$< \Delta x'^2_i > = (\int R_{26i}(s)\, \delta_{RMS-i}\, ds)^2 \qquad (12.b)$$

The additive spatial kicks for coherent processes affect the transverse projected emittance according to equation 5. Then, the emittance growth is a simple matter to calculate.

Transient State Regime

We now account for the transient effects of the CSR self-interaction as the beam is entering and exiting the magnet. The phenomena can be described with two wakefield equations [22, 23]:

$$\frac{dE}{ds}(z, \phi) = W_{ENTERING}(z, \phi) =$$

$$-\frac{4}{R\phi}\lambda(z - S_L) + \frac{4}{R\phi}\lambda(z - 4S_L) -$$

$$\frac{2}{(3R^2)^{\frac{1}{3}}}\int \frac{d}{dz'}[\lambda(z')]\left(\frac{1}{(z-z')^{\frac{1}{3}}}\right)dz' \qquad (13)$$

where z is the coordinate along the bunch, R is the bending radius of the magnet, ϕ is the angle traversed into the magnet by the bunch, λ is the normalized linear charged density, and S_L is the slippage length $(\frac{R\phi^3}{24})$, and

$$\frac{dE}{ds}(z, x, \psi) = W_{EXITING}(z, x, \psi) =$$

$$\frac{4}{R}\frac{\lambda\left(z - \frac{R\emptyset_M^3}{24}\left[\frac{\phi_M + 4x}{\phi_M + x}\right]\right)}{\phi_M + 2x} +$$

$$\frac{4}{R}\left[\int \frac{d}{dz'}[\lambda(z)]\left(\frac{1}{\psi + 2x}\right)dz'\right] \qquad (14)$$

where x is the position of the bunch past the exit of the bending magnet (the observed time) and ψ is the angle of the bunch at which the radiation was emitted (the retarded time). The wakefields are complicated in their dependence of ϕ and ψ when comparing them to the steady state form.

The RMS energy spread throughout the bunch can then be found:

$$\sigma_{W_i} = \left[\int_{-\sigma_z}^{+\sigma_z}[W_i(z)]^2\lambda(z)dz - <W_i(z)>^2\right]^{1/2} \qquad (15)$$

where $W_i(z)$ is either the entering or exiting wake and $<W_i(z)> = \int_{-\sigma_z}^{+\sigma_z}W_i(z)\lambda(z)dz$ is simply the mean. Finally, the same procedure for finding the emittance growth from equation 5 can be applied.

For each method, the transverse projected emittance growth at the exit of chicane was calculated while scanning through various values of theta 1, 2 and 3 (and preserving R_{56}) and the results compared with ELEGANT. The results are shown in Figure 8.
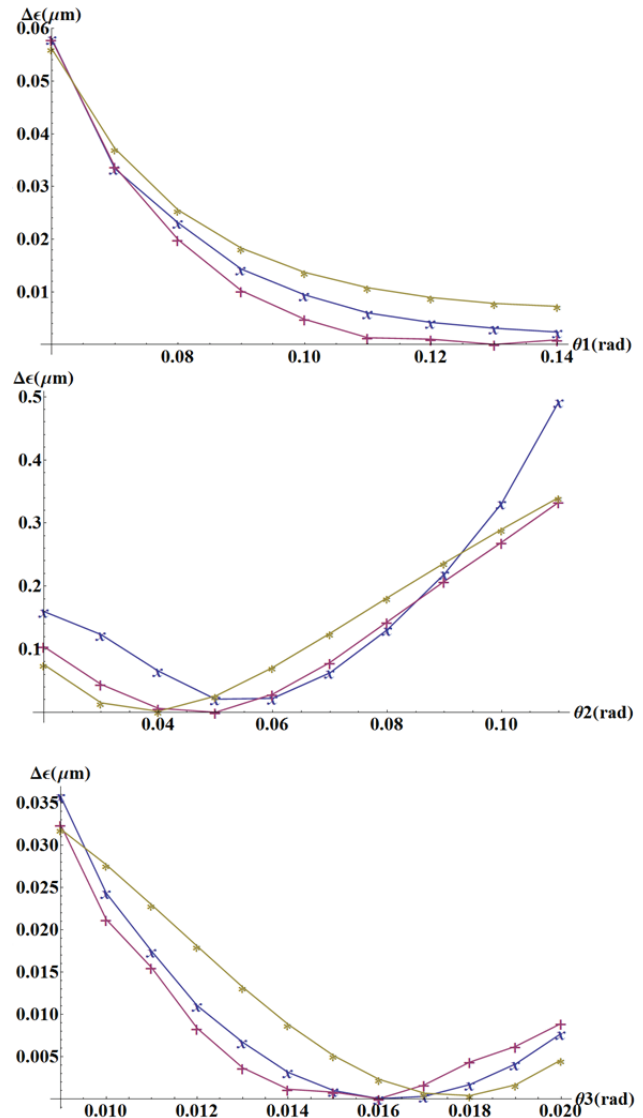
Figure 8: Plots of change in emittance at the exit of the 5-bend chicane for various bend angle scans. For each plot, the "+" is data collected with ELEGANT, the "*" is numerical data using the steady-state linear model, and the "x" is numerical data using the transient-state linear model. Top: Displays the emittance change at the exit of the 5-bend chicane while scanning θ_1. Middle: Displays the emittance change while scanning θ_2. Bottom: Displays the emittance change while scanning θ_3.

The plots above show great agreement between ELEGANT and the steady and transient state linear CSR models. The steady state model is numerically simple to implement and can be calculated with limited resources. While the steady state behaviour agrees well with ELEGANT, we cannot ignore its failure to properly locate the emittance change minimum for scans of θ_2 and θ_3 (Fig. 8). The transient state model, on the other hand, properly locates the emittance change minimum for all angle scans while still maintaining agreement in behavior with ELEGANT. Conversely, the mathematics of the transient state model is far more complicated than that of the steady state. The transient state CSR wakefield

integrals must be evaluated numerically and require considerable resources and computation time.

CONCLUSION

Magnetic bunch compressors are a source of CSR induced emittance growth. New CSR mitigation techniques must be researched and developed to continue pushing X-FEL performance to the forefront.

In this paper, we have introduced a 5-bend chicane as a prospective bunch compressor for final stage compression at LCLS-II. In terms of emittance preservation, the 5-bend chicane is an attractive option with highly reduced CSR emittance growth, and in some cases, full cancellation. We will look to continue researching the 5-bend chicane as, potentially, the new standard in bunch compression and develop its analytical model to the extent of applying its CSR nullification to all relevant bending systems.

ACKNOWLEDGMENT

We would like to extend thanks to Paul Emma, Gennady Stupakov, Lanfa Wang and Mark Woodley for useful discussions.

REFERENCES

[1] M. Borland, "Elegant: A Flexible SDDS-Compliant Code for Accelerator Simulation," Advanced Photon Source LS-287, September 2000.

[2] N. Rohringer, D. Ryan, R. London, M. Purvis et al.,Nature (London) 481, 488 (2012).

[3] H. N. Chapman, P. Fromme, A. Barty, T. A. White, R. A.Kirian et al., Nature (London) 470, 73 (2011).

[4] M. M. Seibert, E. T., F. Maia, M. Svenda et al., Nature (London) 470, 78 (2011).

[5] Raubenheimer, Tor. "LCLS-II Parameters". LCLSII-1.1-PR-0133-R0.

[6] Huang, Zhirong. "Brightness And Coherence Of Synchrotron Radiation And FELs", SLAC-PUB 15449.

[7] W. Ackermann, G. Asova, V. Ayvazyan, A. Azima, N. Baboi, J. Ba¨hr, V. Balandin, B. Beutner, A. Brandt, A.Bolzmann et al., Nat. Photonics 1, 336 (2007).

[8] T. Ishikawa, H. Aoyagi, T. Asaka et al., Nat. Photonics 6, 540 (2012).

[9] Y. S. Derbenev, E. L. S. J. Rossbach, and V. D. Shiltsev, Microbunch Radiative Tail-Head Interaction, Tech. Rep. TESLA-FEL 95-5, Deutsches Elektronen-Synchrotron, Hamburg, Germany (Sep 1995).

[10] Microbunches Workshop, E.B. Blum, M Deines and J.B. Murphy, AIP Conf. Proc. No. 367 (1996).

[11] Z. Huang, J. Wu, T. Shaftan. "Microbunching Instability Due To Bunch Compression". SLAC-PUB-11597. Dec. 2005.

[12] S. Di Mitri, M. Cornacchia, and S. Spampinati, Phys. Rev. Lett. 110, 014801 (2013).

[13] S. Di Mitri, M. Cornacchia. "Merit Functions For The Linac Optics Design For Colliders & Light Sources". NIMA 735, (2014) 60-65.

[14] T. Raubenheimer, P. Emma, S. Kheifets, "Chicane and Wiggler Based Bunch Compressors for Future Linear Colliders", Proc. of 1993 IEEE PAC, Washington D.C. (1993) 635.

[15] Y. Jing, Y. Hao, V.N. Litvinenko. "Compensating Effect of the Coherent Synchrotron Radiation in Bunch Compressors". Phys. Rv. ST Accel. Beams 16, 060704, June 2013.

[16] P. Emma, V. Bharadwaj, Bunch Compressor Options for the LEUTL Facility at the APS, June 1999, unpublished.

[17] M. Borland, J. W. Lewellen, S. V. Milton, "A highly flexible bunch compressor for the APS LEUTL FEL", in proceedings of LINAC2000, Monterey, USA, August 2000.

[18] P. Emma, R. Brinkmann. "Emittance Dilution Through Coherent Energy Spread In Bend Systems". SLAC-PUB-7554, May 1997.

[19] Raubenheimer, Tor. Private communications.

[20] Amann, John. Private communications.

[21] Wang, Lanfa. Private communications.

[22] E. L. Saldin, E. A. Schneidmiller, and M. V. Yurkov, Nuclear Instruments and Methods, Sec. A 398, 373, 1997.

[23] G. Stupakov, P. Emma. "CSR Wake For A Short Magnet In Ultra-Relativistic Limit". LCLS-TN-01-12, Dec. 2001.